ROYAL SOCIETY
OF CHEMISTRY

PAPER

Check for updates

Degradation of three β-O-4 lignin model compounds *via* organic electrolysis and elucidation of the degradation mechanisms†

Yoshiyuki Uruma, [ID] *[a] Tomohiro Yamada,[b] Tsubasa Kojima,[a] Tianyuan Zhang, [ID] [b] Chen Qu,[c] Moe Ishihara,[a] Takashi Watanabe, [ID] [c] Kan Wakamatsu [ID] [d] and Hirofumi Maekawa [ID] [b]

Woody biomass comprising cellulose, hemicellulose, and lignin has been the focus of considerable attention as an alternative energy source to fossil fuel for various applications. However, lignin has a complex structure, which is difficult to degrade. Typically, lignin degradation is studied using β-O-4 lignin model compounds as lignin contains a large number of β-O-4 bonds. In this study, we investigated the degradation of the following lignin model compounds *via* organic electrolysis: 2-(2-methoxyphenoxy)-1-(4-methoxyphenyl)ethanol **1a**, 1-(3,4-dimethoxyphenyl)-2-(2-methoxyphenoxy)-1,3-propanediol **2a**, and 1-(4-hydroxy-3-methoxyphenyl)-2-(2-methoxyphenoxy)-1,3-propanediol **3a**. The electrolysis was conducted for 2.5 h at a constant current of 0.2 A using a carbon electrode. Various degradation products such as 1-phenylethane-1,2-diol, vanillin, and guaiacol were identified upon separation *via* silica-gel column chromatography. The degradation reaction mechanisms were elucidated using electrochemical results as well as density functional theory calculations. The results suggest that the organic electrolytic reaction can be used for the degradation reaction of a lignin model with β-O-4 bonds.

1. Introduction

Petroleum resources have been widely used for various applications ever since the Industrial Revolution. However, owing to the depletion of oil reserves and climate change, the demand for sustainable energy resources to replace oil is increasing.[1] Woody biomass, a general term for cellulose, hemicellulose, and lignin, which make up the cell walls of plants, is a naturally abundant chemical resource and common alternative to petroleum (Fig. 1). If explored *via* nanotechnology, lignocellulosic biomass (LCB) can be refined to yield high-performance fuel sources. The toxicity and cost of conventional methods can be reduced by applying nanoparticles in the refining of LCB.[2] It can be used for manufacturing value-added chemicals and fuels and facilitates industrial production from renewable

biomass, known as "biorefinery," named after "oil refinery" (industrial production from petroleum resources).[3]

However, the complex structure of woody biomass makes its applications challenging. Efficient lignin degradation is required for effectively using woody biomass. Lignin has a complex structure of C–C bonds or C–O bonds in phenylpropane units such as syringyl, guaiacyl, and hydroxyphenyl (Table 1).[4]

The β-O-4 bond is characteristic of lignin, and many studies have been conducted on the oxidative lignin degradation of the β-O-4 bonds in lignin.[5] For example, lignin peroxidase, manganese peroxidase, and laccase isolated from white-rot fungi are lignin-degrading enzymes. Lignin degradation by lignin peroxidase reduces methylated lignin and cleaves the Cα–Cβ bond in the side chain.[6,7]

Nonaka *et al.* used a different method for the β-O-4 bond cleavage. They subjected lignin to organic electrolytic reactions under mild conditions without special reagents or catalysts and reported four types of oxidative degradation products (Fig. 2). They also concluded that the generation of a single product is difficult and that a robust method for the separation of the degradation products is essential.[8] For example, thermochemical decomposition of lignin using a catalyst and internal heating, which are energy-saving and mild conditions, resulted in low yield and lack of reaction selectivity (Fig. 3).[9]

[a]Department of Integrated Engineering, Chemistry and Biochemistry Division, National Institute of Technology, Yonago College, 4448, Hikona-cho, Yonago City, Tottori 683-8502, Japan. E-mail: uruma@yonago-k.ac.jp

[b]Department of Materials Science and Technology, Nagaoka University of Technology, 1603-1, Kamitomioka-cho, Nagaoka, Niigata 940-2188, Japan

[c]Research Institute for Sustainable Humanosphere, Kyoto University, Gokasho, Uji, Kyoto 611-0011, Japan

[d]Department of Chemistry, Faculty of Science, Okayama University of Science, 1-1 Ridaicho, Kita-ku, Okayama 700-0005, Japan

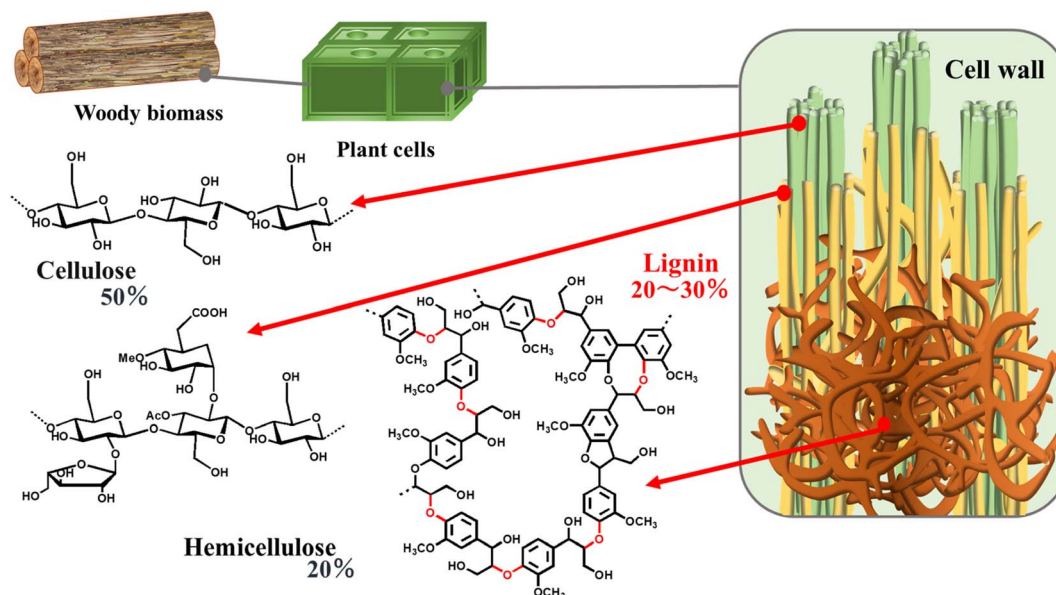† Electronic supplementary information (ESI) available. See DOI: https://doi.org/10.1039/d3ra02486e

Fig. 1 Components of woody biomass.

Table 1 Lignin model compounds bearing the β-O-4 bond

1a

2-(2-Methoxyphenoxy)-1-(4-methoxyphenyl)ethanol

2a

1-(3,4-Dimethoxyphenyl)-2-(2-methoxyphenoxy)-1,3-propanediol

3a

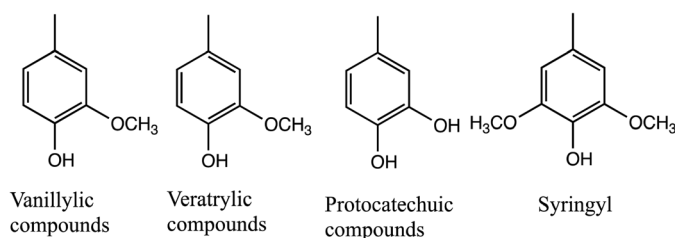1-(4-Hydroxy-3-methoxyphenyl)-2-(2-methoxyphenoxy)-1,3-propanediol

Vanillylic compounds

Veratrylic compounds

Protocatechuic compounds

Syringyl compounds

Fig. 2 Four types of oxidative degradation products of lignin.

Gao *et al.* investigated β-O-4 lignin model compounds *via* electrochemical oxidation with an iodide ion mediator. They used 2,2-dimethoxy-2-arylacetaldehyde as a β-O-4 lignin model to investigate the electrochemical selective C–O bond cleavage.[10] In this study, we analyzed the lignin degradation products of the following β-O-4-type lignin model compounds

via constant current electrolysis: 2-(2-methoxyphenoxy)-1-(4-methoxyphenyl)ethanol **1a**, 1-(3,4-dimethoxyphenyl)-2-(2-methoxyphenoxy)-1,3-propanediol **2a**, and 1-(4-hydroxy-3-methoxyphenyl)-2-(2-methoxyphenoxy)-1,3-propanediol **3a**. The experimental conditions (solvent, supporting salt, and electrodes) without additives were optimized. The degradation products were isolated using silica-gel column chromatography and the degradation mechanisms were elucidated *via* GC-MS analysis and density functional theory (DFT) calculations.

2. Results and discussion

2.1. β-O-4 model compounds

Lignin has a complex structure with a large number of β-O-4 bonds and, therefore, its degradation mechanism is typically studied using model compounds. 2-Aryloxyl-aryl ethanol is commonly used as a lignin model compound.[11] Several studies on the degradation of lignin models *via* electrolysis have been conducted. Pardini *et al.* reported the electrolytic oxidation of a dimeric lignin model.[12] In this study, 2-(2-methoxyphenoxy)-1-(4-methoxyphenyl)ethanol **1a** was used as the primary lignin model compound. In addition, 1-(3,4-dimethoxyphenyl)-2-(2-methoxyphenoxy)-1,3-propanediol **2a** and 1-(4-hydroxy-3-methoxyphenyl)-2-(2-methoxyphenoxy)-1,3-propanediol **3a**, which has similar structures to that of lignin, were used for the electrolysis experiments. Compound **1a** was synthesized in two steps using a previously reported method (Scheme 1).[10]

2.2. Organic electrolysis

Organic electrolytic reactions are pollution-free, energy-saving, and resource-saving and, thus, have attracted attention as clean chemical reactions occurring at the electrodes.[13] Therefore, we chose this method for lignin degradation to establish a method that promotes the use of lignocellulosic biomass as
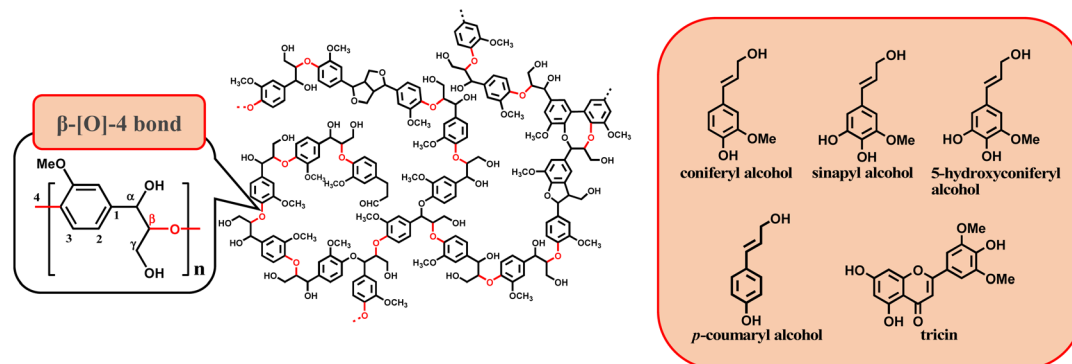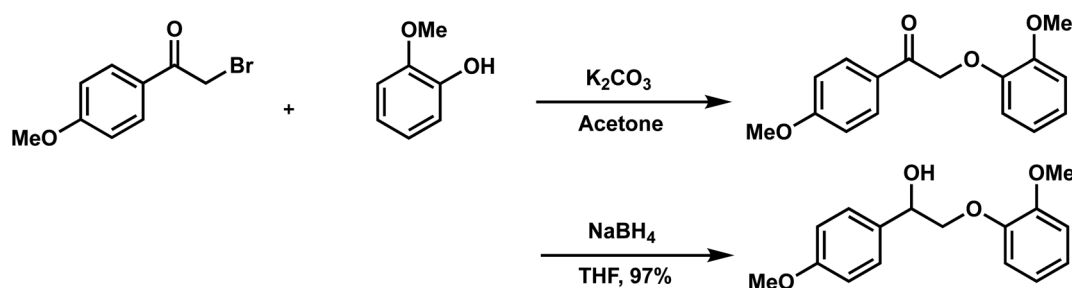
Fig. 3 Lignin structure (left) and β-O-4 model compounds (right).

Scheme 1 Synthesis of **1a**.

a clean energy source. Several studies on lignin electrolysis have been previously reported. Li *et al.* reported the catalytic electrochemical degradation of aspen lignin in a three-dimensional electrode reactor using Pb/PbO$_2$ anodes.[14] Zang *et al.* demonstrated selective and efficient oxidation of the Cα–Cβ bond in 2-phenoxy-1-phenyl ethanol, a typical β-O-4 lignin model compound, utilizing multiphase active interfaces and smooth pore channels; a degradation rate of 93.6% and benzoic acid yield of 83.8% were reported.[15]

Organic electrolysis reactions entail electron transfer (E process) and chemical reactions (C process). The product is obtained *via* an intermediate E process. Therefore, the selection of solvent and electrode is important.[16] When a carbon (C) electrode was used, precipitates adhered to the electrode after 2 hours of electrolysis, and subsequent processes, such as an increase in voltage and electrolytic reaction temperature, were observed (Table 2).

The endpoint of the reaction was set at 2.5 hours when the lignin model compound was used as much as possible in the reaction and disappeared, and the electrolysis reaction could be performed stably.

The reason why a little methanol was added to the electrolysis reaction was to suppress the increase in voltage (Fig. 4).

Therefore, 2.5 hours was considered optimal for electrolysis. The reaction was monitored by thin layer chromatography (TLC), which confirmed the complete degradation of the lignin model compound detected at Rf 0.22 (EtOAc/hexane 1 : 3), with a new spot appearing at Rf 0.00 that appeared to be a degradation product (Fig. 5).

After each electrolysis, the electrode was checked, deposits were removed, and the electrode was polished. The thickness of the electrode was also measured after each electrolysis, and it was found that the electrode was corroded by about 0.1 mm after one reaction.

Table 2 Relationship between solution temperature and voltage during electrolysis

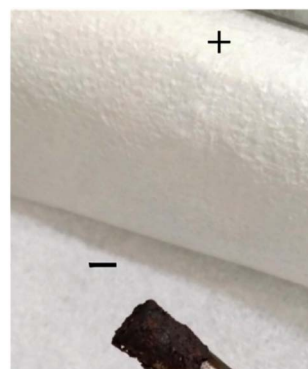| Time (h)	0	0.5	1	1.5	2	2.5	3
Voltage (V)	17	17	17	19	20	27	45
Temperature (°C)	22	25	26	28	28	30	33

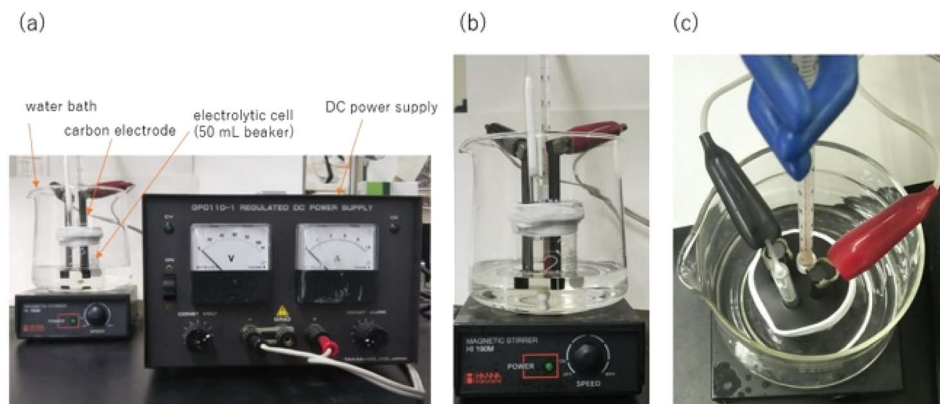**Fig. 4** The electrode after the electrolytic reaction.

Fig. 5 (a) Setup of the electrolysis equipment: DC power supply, carbon electrode, and electrolytic cell; (b) side-view and (c) top-view of the electrolysis cell.

2.3. Organic electrolysis of 1a, 2a, and 3a

Electrolysis of the lignin models **1a**, **2a**, and **3a** required the use of tetraethylammonium *p*-toluenesulfonate (Et₄NOTs) as the supporting electrolyte.

Initially, complete degradation of the raw materials was attempted. However, the reaction voltage increased because of the residues on the electrodes and, consequently, the temperature of the reaction solution increased. A stable electrolytic reaction was observed for only 2.5 h. The depth of immersion of the electrodes was varied to suppress the increase in the reaction temperature under mild reaction conditions. In the initial phase of the reaction, the solution in the electrolytic cell, which was initially colorless and transparent, turned brown. After extraction with ethyl acetate, the solvent was distilled under reduced pressure to afford a brown oily electrolyte mixture. The electrolyte was a mixture containing multiple components, and the degradation products were confirmed by TLC using a developing solvent of ethyl acetate : hexane = 1 : 2 with 1% acetic acid. Furthermore, electrolytic reactions of **2a** and **3a**, which have comparable structures to that of lignin, were performed. Guaiacol was isolated from **2a** and its degradation reaction rate was 75% using CH₃OH/CH₃CN. In contrast, guaiacol and vanillin were isolated from **3a** at a degradation rate of 65% (Table 3).

The assignment of degradation products were evaluated using ¹H NMR spectroscopy and GC-MS. The cylindrical C electrode had a diameters of 0.8 cm. The plate Pt electrode has a size dimension of 20 mm × 10 mm × 0.5 mm. The C electrode (SEG-R, Nippon Carbon Co. Ltd) was immersed in the reaction solution at a depth of 1.2 cm from the surface. The reaction was conducted under constant current at a current density of 0.13 A cm⁻². The reaction progression was monitored using TLC, and the products were isolated by silica-gel column chromatography. The degradation rate was calculated using eqn (1):

$$\text{Conversion rate}(\%) = \frac{\text{starting material} - \text{recovered starting material}}{\text{starting material}} \times 100 \quad (1)$$

where the recovered starting material was isolated by silica-gel column chromatography.

In the case of using a Pt electrolyte, even though lignin model compounds degradation occurred, the reaction rate was low when a Pt electrode was used. Moreover, the reaction rate decreased in the absence of acetonitrile (Run 3). For **1a**, the reaction rate was 82% in a mixed methanol/acetonitrile solvent, whereas it was 77% when only methanol was used. This is attributed to the excellent electrolytic oxidation observed in organic solvents with dielectric constants of ≥30.[17] Notably, when the Pt electrode was used, even though the reaction rate was low, the degradation products were clean, and complex degradation products were not observed. This suggests that a large number of degradation products were generated in the electrolytic oxidation under harsh conditions in Runs 1 and 2. However, the structure elucidation of these products was difficult. Furthermore, the electrolytic oxidation of **2a**, which has a similar β-O-4 bond to that in lignin model compound, proceeded at a reaction rate of 87%, and guaiacol was confirmed as a degradation product (Run 4). Similarly, guaiacol and vanillin were detected as the degradation products of **3a** at reaction rates of ≥65% (Runs 6 and 7). The degradation products and samples were purified by silica-gel column chromatography and evaluated by GC-MS. The degradation products of **1a** were determined to be 4-methoxy benzoic acid (B1), 4-methoxy benzaldehyde (B2), and 4-methoxybenzyl alcohol (B4) (Fig. 6).
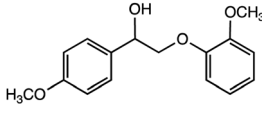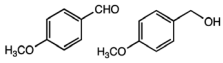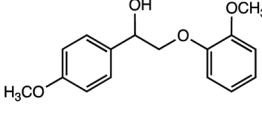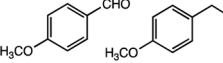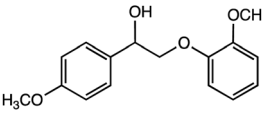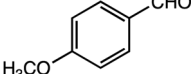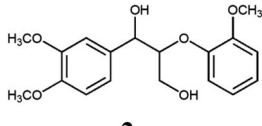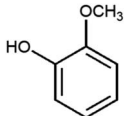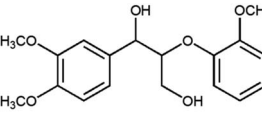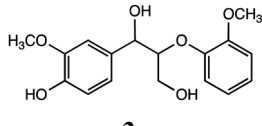
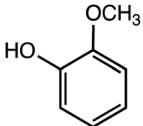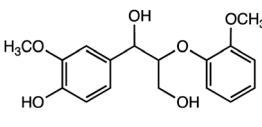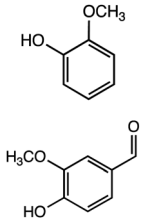Pardini *et al.* reported that the Cα–Cβ bond was cleaved during electrolysis using a mediator, yielding an aldehyde.[12] As the guaiacyl-type benzene ring is electron-rich, cation radical species could be easily generated by a one-electron oxidation reaction. To prove that the guaiacol aromatic rings are more easily oxidized, we conducted cyclic voltammetry tests on **1a** using 1-phenylethane-1,2-diol, 1-(4-methoxy)-ethane-1,2-diol, and 1,2-dimethoxybenzene as the standard materials (Table 4).

The oxidation potentials of **1a** were determined to be 1.47, 1.85, and 2.12 V, indicating that the guaiacyl-type aromatic rings were easily oxidized. This may be attributed to the presence of a methoxy group at the 4-position of the benzene ring. This suggests that a nucleophilic attack on the cationic species

Table 3 Summary of the decomposition reactions during electrolysis of **1a**, **2a**, and **3a**

| Run	Compounds	Electrode	Solvent	Electric current [A]	Current density [A m^{-2}]	Charge [C]	Time [h]	Degradational products	Degradation rate
1	**1a**	C	CH$_3$OH CH$_3$CN	0.2	0.13	1800	2.5		82%
2	**1a**	C	CH$_3$OH	0.2	0.13	1800	2.5		77%
3	**1a**	Pt	CH$_3$OH	0.2	0.10	1800	2.5		66%
4	**2a**	C	CH$_3$OH CH$_3$CN	0.2	0.13	1800	2.5		87%
5	**2a**	C	CH$_3$OH	0.2	0.13	1800	2.5		
6	**3a**	C	CH$_3$OH CH$_3$CN	0.2	0.13	1800	2.5		75%
7	**3a**	C	CH$_3$OH	0.2	0.13	1800	2.5		65%

by MeOH affords an *ortho*-quinone acetal, and the subsequent electrogenerated acid-catalyzed transesterification of the acetal generates 1-(4-methoxyphenyl)ethane-1,2-diol.
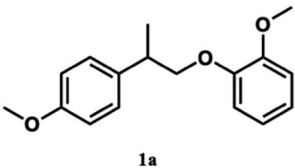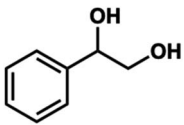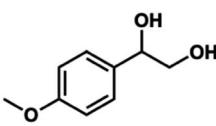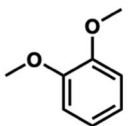
We hypothesized that we could confirm the feasibility of using electrolysis for lignin degradation by investigating the degradation of a structure comparable to that of lignin (**2a** and **3a**). The reactions were evaluated by GC-MS without separation to confirm the degradation products.

The GC-MS analysis of **2a** and **3a** is shown in Fig. 7. The blue and red spectra indicate the reaction electrolysis using Pt and C electrodes, respectively. The product mixture was evaluated by

GC-MS without product isolation. The column temperature was programmed as follows: the temperature was initially maintained at 50 °C for 3 min, then increased at 3 °C min^{-1} to 300 °C and maintained for 7.5 min. In the case of **2a**, guaiacol and methoxyvanillin were detected on both the Pt and C electrodes. When the reaction was performed at 6 F using a C electrode, a small amount of methoxyvanillin was detected, along with the main product guaiacol. Similarly, the decomposition of **3a** yielded guaiacol as the major product, along with a small amount of methoxyvanillin, irrespective of the electrode type.
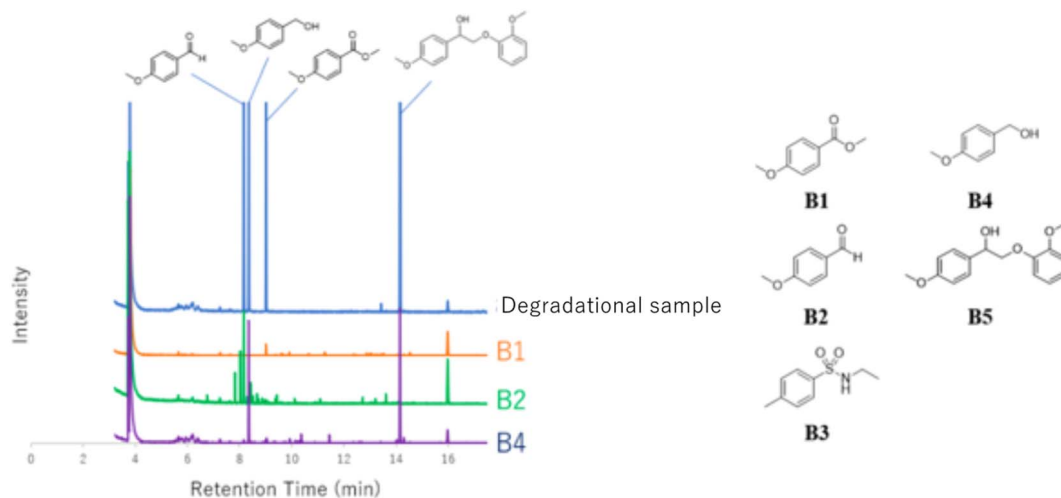
Fig. 6 GC-MS analysis of **1a**.

Table 4 Oxidation potentials of lignin model **1a** and its degradation products[a]

Substrate	Oxidation potentials
1a	1.47 V
	1.85 V
	2.12 V
1-Phenylethane-1,2-diol	2.25 V
	2.81 V
	2.81 V
1-(4-Methoxyphenyl)ethane-1,2-diol	1.69 V
	2.08 V
1,2-Dimethoxybenzene	1.05 V
	1.70 V
	2.12 V

[a] Working electrode: Pt; counter electrode: Pt; reference electrode: Ag/AgCl; solvent: MeCN; supporting electrolyte: 0.1 M n-Bu$_4$NClO$_4$; scan rate: 0.2 V s^{-1}.
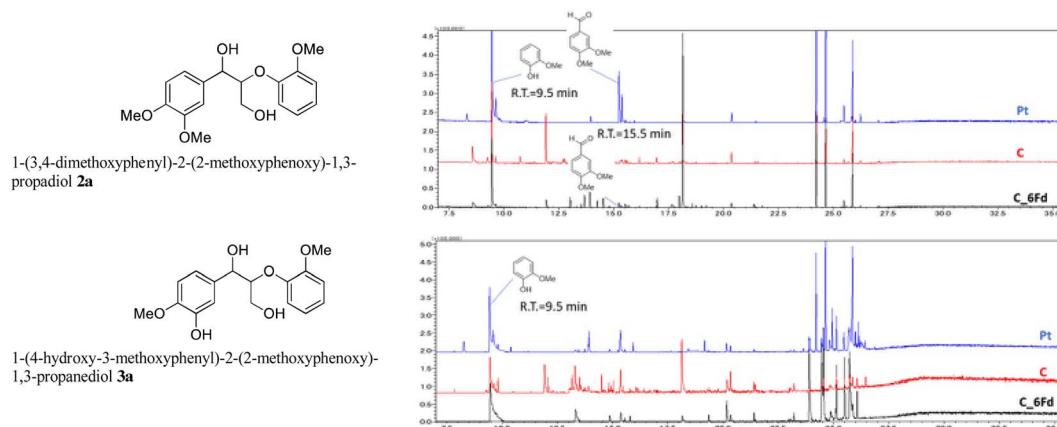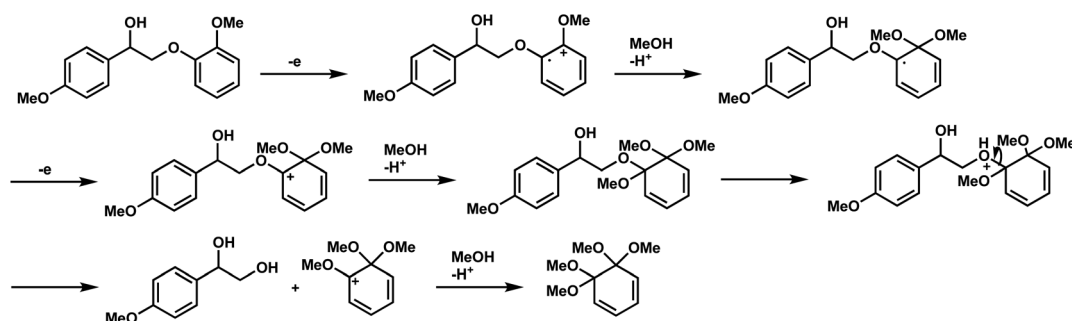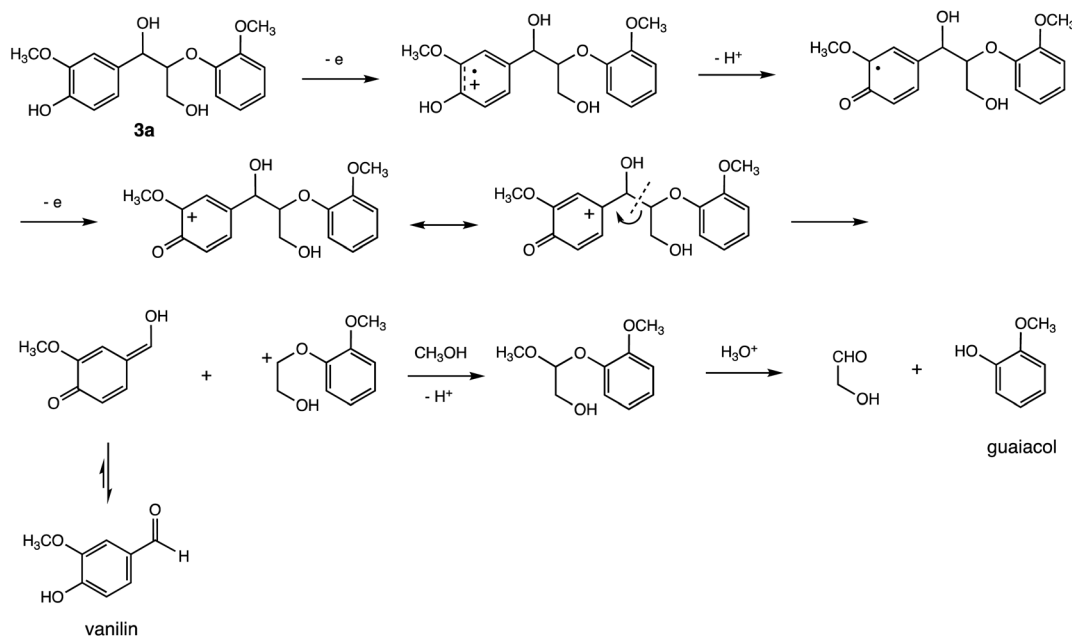
The degradation mechanism of **3a** is shown in Scheme 3. Oxidation of the phenolic hydroxyl group to the quinone form leads to C–C bond cleavage owing to the electron transfer from the benzyl position. However, the intermediates have not yet been identified. Moreover, the easily oxidizable portion in **2a** was difficult to identify, thus limiting our ability to elucidate its degradation mechanism. Therefore, computational studies were conducted.

The proposed degradation mechanism for **1a** is outlined in Scheme 2. To gain more insight into the mechanism, DFT calculations were performed at the B3LYP/6-31G(d) level using the Gaussian 16 program.[18] The natural population analysis[19] of the radical cation of **1a** (**1a·+**) revealed that both charge and spin were nearly localized in the guaiacyl-type aromatic moiety (+0.95 for charge and 1.00 for spin in conformer 1, see Fig. S1 and S2†). Because the nucleophilic attack of MeOH may occur at several positions on the guaiacyl moiety, the elucidation of the degradation mechanism is challenging (see Scheme S1 and Table S1†). However, 1-(4-methoxyphenyl)-1,2-ethanediol or its 2-methyl ether derivative is produced as a common intermediate at a sufficiently low oxidation potential. The 1,2-diol derivative was immediately oxidized to 4-methoxybenzaldehyde and methyl 4-methoxybenzoate. 4-Methoxybenzyl alcohol was likely formed via hydrogen transfer from the MeOH adduct of the aldehyde radical cation to the neutral form of the aldehyde; however, further investigation is required (Scheme 4).

The proposed degradation mechanisms of **2a** and **3a** are outlined in Schemes 5 and 3. Both charge and spin of the radical cations of **2a** (**2a·+**) and **3a** (**3a·+**) are mainly distributed in the 3,4-dimethoxybenzylic or 3-methoxy-4-hydroxybenzylic moiety (+0.81 (**2a·+**) and +0.66 (**3a·+**) for charge; 0.84 (**2a·+**) and 0.68 (**3a·+**) for spin in conformer 2, see Fig. S1 and S2†). The **2a·+** moiety can react with MeOH to afford **3a·+** and Me$_2$O exergonically ($\Delta G = -6.11$ kcal mol^{-1}). Proton abstraction from the hydroxy group of **3a·+** yields the corresponding neutral radical, which undergoes oxidation to produce the quinoid cation **4$^+$**. The oxonium cationic center would facilitate the cleavage of the central C–C bond to produce **5**, which isomerizes to vanillin and **6$^+$** ($\Delta G = -7.32$ kcal mol^{-1}). Fragment **6$^+$** reacts with MeOH to form an acetal intermediate, which is then hydrolyzed to produce guaiacol.

1-(3,4-dimethoxyphenyl)-2-(2-methoxyphenoxy)-1,3-propadiol **2a**

1-(4-hydroxy-3-methoxyphenyl)-2-(2-methoxyphenoxy)-1,3-propanediol **3a**

Fig. 7 GC-MS analysis of **2a** and **3a**.

Scheme 2 Proposed degradation mechanism of **1a**.

guaiacol

vanilin

Scheme 3 Degradation mechanism of **3a** and formation of vanillin and guaiacol.
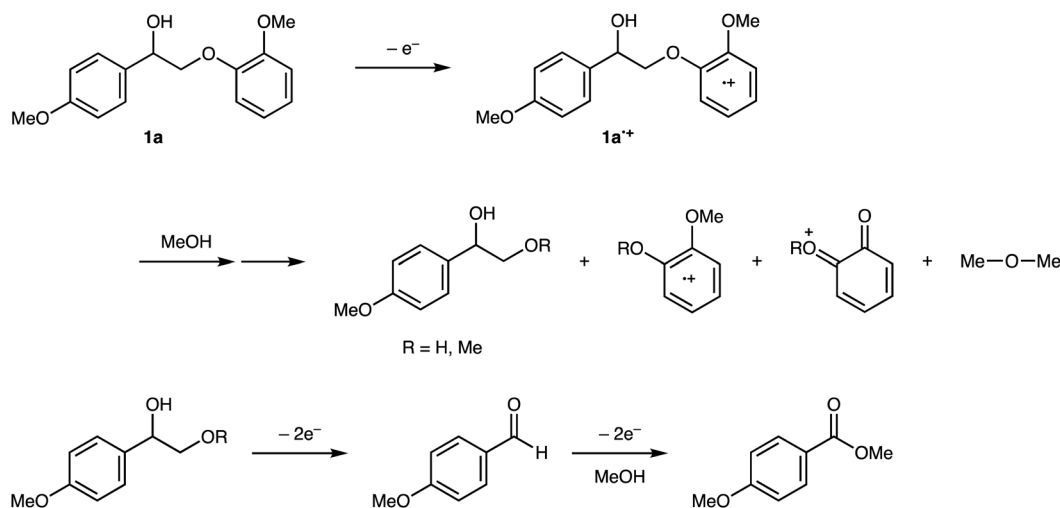
Scheme 4 Degradation mechanism of **1a** elucidated *via* DFT calculations.
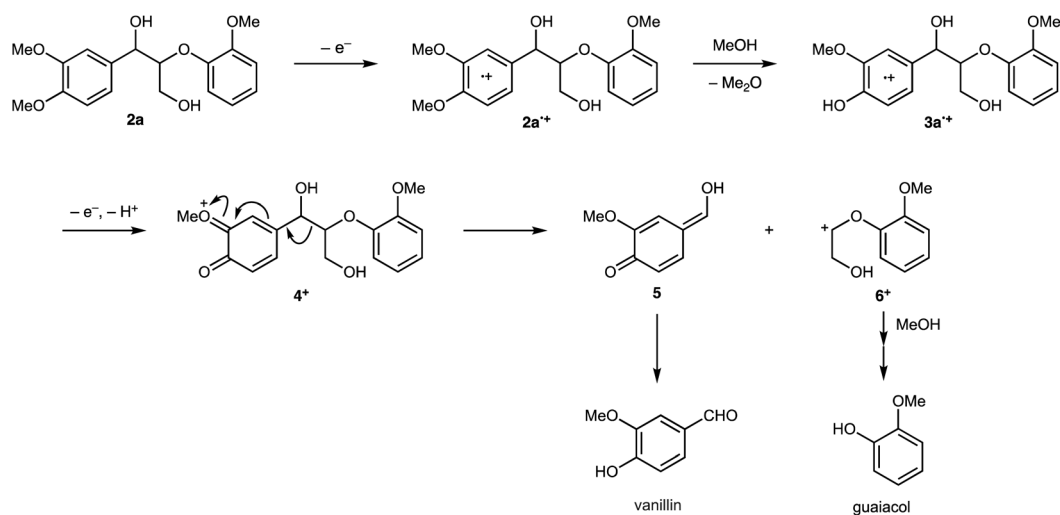
Scheme 5 Degradation mechanism of **2a** elucidated *via* DFT calculations.

3. Conclusion

In this study, we investigated the degradation of lignin model compounds 2-(2-methoxyphenoxy)-1-(4-methoxyphenyl)ethanol **1a**, 1-(3,4-dimethoxyphenyl)-2-(2-methoxyphenoxy)-1,3-propanediol **2a** and 1-(4-hydroxy-3-methoxyphenyl)-2-(2-methoxyphenoxy)-1,3-propanediol **3a** *via* electrolysis. The optimal degradation duration was 2.5 h. Methoxyvanillin, benzaldehyde, and 1-phenylethane-1,2-diol were identified as the degradation products of **1a**, whereas guaiacol and vanillin were the degradation products of **2a** and **3a**. Duan *et al.* reported reactions using a Pt electrode and tBuOOH as an oxidant to obtain lignin model dimers, polymeric compounds, and even natural lignin as the desired aromatic aldehyde.[20] We also proposed degradation mechanisms for **1a**, **2a**, and **3a** based on GC-MS analysis and DFT calculations. This study used carbon and platinum electrodes to degrade lignin model compounds. It

was found that useful products were obtained at high degradation rates without oxidants.

This new finding differs from previous reports of electrolytic reactions with oxidants. Investigation into the applications of these degradation products is currently underway.

4. Experimental

4.1. Instruments and reagents

^{1}H and ^{13}C NMR spectra were recorded on a BRUKER 400 instrument at 400 and 100 MHz, respectively. The chemical shifts are reported as δ values in relation to the internal standards tetramethylsilane (0 ppm) and CHCl$_3$ (77.0 ppm) for ^{1}H and ^{13}C NMR spectra, respectively. High-resolution mass spectra (HRMS) were obtained using JMS-AX 500 and JMS-700T spectrometers at the Analytical Center of Osaka City University. Silica gel (silica gel 60, 230–400 mesh) was used for flash chromatography. Pre-coated silica gel plates (Merck 5715 and

60F254) were used for TLC. 2-(2-Methoxyphenyl)oxy-1-phenetanol, which was used as the starting material for OEM, was synthesized using a previously reported method. Carbon electrode (SEG-R; Nippon Carbon Co., Ltd) was purchased from TCI. 1-(3,4-Dimethoxyphenyl)-2-(2-methoxyphenoxy)-1,3-propanediol **2a** was purchased from Wako. 1-(4-Hydroxy-3-methoxyphenyl)-2-(2-methoxyphenoxy)-1,3-propanediol **3a** was purchased from TCI.

4.2. Preparation of β-O-4 lignin model

We prepared the β-O-4 lignin model 2-(2-methoxyphenyl)oxy-1-phenethanol using a method previously reported by Nichols at al.[8]

4.3. Organic electrolysis

A 50 mL beaker cell was equipped with a carbon electrode, thermometer, and DC-regulated power supply. Lignin model substrate (0.2 g; 0.82 mmol), tetraethylammonium p-toluene-sulfonate (1.0 g; 3.32 mmol), 1.5 mL of methanol, and 28.5 mL of acetonitrile were added to the cell. The mixture was electrolyzed under constant current at 0.2 A for 2.5 h with continuous stirring and cooling in a water bath. After electrolysis, the mixture was extracted with ethyl acetate (50 mL × 3). The organic phase was washed with brine and dried over Na_2SO_4. The organic extracts were then concentrated under reduced pressure. The residue was subjected to column chromatography to separate the products.

4.4. Degradation products

The degradation mixture obtained from organic electrolysis was separated and purified using silica-gel column chromatography (ethyl acetate : hexane = 1 : 2, 1% acetic acid). Six degradation products were obtained by distilling the solvent at reduced pressure for each fraction. These products were further purified by preparative TLC, and their structures were determined by NMR and mass spectrometry. GC-MS measurements were used to evaluate lignin models **2a** and **3a**. A GCMS-QP2010SE instrument (Shimadzu, Kyoto, Japan) was connected to a DB-5MS column (30 m × 0.25 mm id, 0.25 μm film thickness; Agilent Technologies). MS measurements were performed in the electron ionization mode at a voltage of 0.7 eV. The MS scanning range was m/z 30–700. The column temperature was initially maintained at 50 °C for 3 min and then raised to 300 °C at 3 °C min^{-1}, where it was maintained for 7.5 min. The compounds were identified by a GCMS-QP2010SE similarity search.

4.4.1. Benzaldehyde (1). ^{1}H NMR (CDCl$_3$, 600 MHz) δ 7.54 (t, J = 8.1 Hz, 2H), 7.64 (t, J = 7.4 Hz, 1H), 7.89 (d, J = 7.0 Hz, 2H), 10.03 (s, 1H); ^{13}C NMR (CDCl$_3$, 150 MHz) δ 129.00, 129.75, 134.46, 136.49, 192.38.

4.4.2. 1-((Methoxymethoxy)methyl)benzene (2). ^{1}H NMR (CDCl$_3$, 600 MHz) δ 3.42 (s, 3H), 4.60 (s, 2H), 4.72 (s, 2H), 7.36 (t, 4.8 Hz, 2H), 7.363 (d, J = 4.8 Hz, 2H), 7.47 (t, J = 7.8 Hz, 1H); ^{13}C NMR (CDCl$_3$, 150 MHz) 55.35, 69.19, 95.68, 126.67, 127.89, 128.56, 137.84; HRMS (FAB, pos) m/z 151.1003 (calcd for C$_9$H$_{11}$O$_2$, 151.0759 [M − H]$^+$).

4.4.3. Methyl 4-(2-acetoxyethyl)benzoate (3). ^{1}H NMR (CDCl$_3$, 600 MHz) δ 2.04 (s, 3H), 2.94 (t, J = 7.0 Hz, 2H), 3.76 (s, 3H), 4.28 (t, J = 7.1 Hz, 2H), 5.99 (dd, J = 8.1, 2.3 Hz, 2H), 7.90 (dd, J = 8.0, 2.3 Hz, 2H); ^{13}C NMR (CDCl$_3$, 150 MHz) δ 20.99, 35.08, 51.52, 64.92, 123.89, 137.98, 141.00, 166.06, 171.00; HRMS (FAB, pos) m/z 221.0819 (calcd for C$_{12}$H$_{13}$O$_4$, 221.0814 [M − H]$^+$).

4.4.4. 1-Phenylethane-1,2-diol (4). ^{1}H NMR (CDCl$_3$, 600 MHz) δ 2.64 (s, 1H), 3.06 (s, 1H), 3.64 (dd, J = 11.4, 8.4 Hz, 1H), 3.74 (dd, J = 11.4, 3.4 Hz, 1H), 4.80 (dd, J = 8.3, 1.5 Hz, 1H), 7.29 (t, J = 4.8 Hz, 1H), 7.35 (d, J = 4.8 Hz, 4H); ^{13}C NMR (CDCl$_3$, 150 MHz) δ 68.04, 74.65, 126.03, 127.93, 128.48, 140.47; HRMS (FAB, pos) m/z 138.0684 (calcd for C$_8$H$_{10}$O$_2$, 138.0675 [M]$^+$).

4.5. DFT calculations

Calculations were performed using the Gaussian 16 program package.[18] The structures of the closed-shell species were optimized at the restricted B3LYP/6-31G(d) level, whereas the structures of open-shell species (**1a˙+**, **2a˙+**, and **3a˙+**) were optimized using the unrestricted theory at the same level. Frequency analysis was performed for each optimized structure to confirm that no imaginary frequencies were obtained for the energy-minimum structures. These calculations were performed in an MeOH solution using a polarizable continuum model. A built-in Gaussian natural population analysis was used to estimate the charge and spin distributions.[19]

Conflicts of interest

The authors declare no conflict of interest.

Acknowledgements

References

1 V. A. Rebecca, V. Ruben, S. Véronique, C. M. Jennife, D. Paul and B. Wout, *Biotechnol. Bioeng.*, 2013, **6**, 64.

2 N. Dey, G. Kumar, A. S. Vickram, M. Mohan, R. R. Singhania, A. K. Patel, C. D. Dong, K. Anbarasu, S. Thanigaivel and V. K. Ponnusamy, *Bioresour. Technol.*, 2022, **344**(Pt A), 126171.

3 G. Chatel and R. D. Rogers, *ACS Sustainable Chem. Eng.*, 2014, **2**, 322–339.

4 G. Zhu, X. Qiu, Y. Zjao, Y. Qian, Y. Pang and X. Ouyang, *Bioresour. Technol.*, 2016, **218**, 718–722.

5 (*a*) Y. Liu, Q. Luo, Q. Qiang, H. Wang, Y. Ding, C. Wang, J. Xiao, C. Li and T. Zhang, *ChemSusChem*, 2022, **15**(21), e202201401; (*b*) C. Scimmi, L. Sancineto, J. Drabowicz and C. Santi, *Int. J. Mol. Sci.*, 2022, **23**(8), 4378.

6 M. Tien and T. K. Kirk, *Science*, 1983, **221**, 661–663.

7 J. K. Glenn, M. A. Morgan, M. B. Mayfield, M. Kuwahara and M. H. Gold, *Biochem. Biophys. Res. Commun.*, 1983, **114**, 1077–1083.

8 A. A. Yoshiyama, T. Fuchigami, T. Nonaka, T. C. Chou and H. J. Tien, *Chem. Express*, 1986, **1**, 212.

9 A. Ashutosh, R. Masud and P. Jeong-Hun, *Fuel Process. Technol.*, 2018, **181**, 115–132.

10 (*a*) W.-J. Gao, C. M. Lam, B.-G. Sun, R. D. Little and C.-C. Zeng, *Tetrahedron*, 2017, **73**, 2447–2454; (*b*) A. Yoshiyama, T. Fuchigami, T. Nonaka, T.-C. Chou and H.-J. Tien, *Chem. Express*, 1986, **1**, 212.

11 J. M. Nichols, L. M. Bishop, R. G. Bergman and J. A. Ellman, *J. Am. Chem. Soc.*, 2010, **132**, 12554–12555.

12 V. L. Pardini, C. Z. Smith, J. H. P. Utley, R. R. Vargas and H. Viertler, *J. Org. Chem.*, 1991, **56**, 7305–7313.

13 S. Rodrigo, D. Gunasekera, J. P. Mahajan and L. Luo, *Curr. Opin. Electrochem.*, 2021, **28**, 100712.

14 Y. S. Wang, F. Yang, Z. H. Liu, L. Yuan and G. Li, *Catal. Commun.*, 2015, **67**, 49–53.

15 N. Wang, R. Xue, N. Yang, H. Sun, B. Zhang, Z. Ma, Y. Ma and L. Zang, *J. Alloys Compd.*, 2022, **929**, 167324.

16 Y. Liu, C. Li, W. Miao, W. Tang, D. Xue, C. Li, B. Zhang, J. Xiao, A. Wang, T. Zhang and C. Wang, *ACS Catal.*, 2019, **9**, 4441–4447.

17 N. L. Weinberg and H. R. Weinberg, *Chem. Rev.*, 1968, **68**, 449.

18 M. J. Frisch, G. W. Trucks, H. B. Schlegel, G. E. Scuseria, M. A. Robb, J. R. Cheeseman, G. Scalmani, V. Barone, G. A. Petersson, H. Nakatsuji, X. Li, M. Caricato, A. V. Marenich, J. Bloino, B. G. Janesko, R. Gomperts, B. Mennucci, H. P. Hratchian, J. V. Ortiz, A. F. Izmaylov, J. L. Sonnenberg, D. Williams-Young, F. Ding, F. Lipparini, F. Egidi, J. Goings, B. Peng, A. Petrone, T. Henderson, D. Ranasinghe, V. G. Zakrzewski, J. Gao, N. Rega, G. Zheng, W. Liang, M. Hada, M. Ehara, K. Toyota, R. Fukuda, J. Hasegawa, M. Ishida, T. Nakajima, Y. Honda, O. Kitao, H. Nakai, T. Vreven, K. Throssell, J. A. Montgomery Jr, J. E. Peralta, F. Ogliaro, M. J. Bearpark, J. J. Heyd, E. N. Brothers, K. N. Kudin, V. N. Staroverov, T. A. Keith, R. Kobayashi, J. Normand, K. Raghavachari, A. P. Rendell, J. C. Burant, S. S. Iyengar, J. Tomasi, M. Cossi, J. M. Millam, M. Klene, C. Adamo, R. Cammi, J. W. Ochterski, R. L. Martin, K. Morokuma, O. Farkas, J. B. Foresman and D. J. Fox, *Gaussian 16, Revision C.01*, Gaussian, Inc., Wallingford CT, 2016.

19 E. D. Glendening, A. E. Reed, J. E. Carpenter and F. Weinhold, *The Gaussian Package Includes the Program of Natural Bond Orbital Analysis: NBO program version 3.1*.

20 L. Ma, H. Zhou, X. Kong, Z. Li and H. Duan, *ACS Sustainable Chem. Eng.*, 2021, **9**, 1932–1940.